

# Anisotropic Coulomb exchange as source of Kitaev and off-diagonal symmetric anisotropic couplings

Pritam Bhattacharyya,<sup>1</sup> Thorben Petersen,<sup>1</sup> Nikolay A. Bogdanov,<sup>2</sup> and Liviu Hozoi<sup>1</sup>

<sup>1</sup>*Institute for Theoretical Solid State Physics, Leibniz IFW Dresden, Helmholtzstraße 20, 01069 Dresden, Germany*

<sup>2</sup>*Max Planck Institute for Solid State Research, Heisenbergstraße 1, 70569 Stuttgart, Germany*

(Dated: July 3, 2023)

Exchange underpins the magnetic properties of quantum matter. In its most basic form, it occurs through the interplay of Pauli’s exclusion principle and Coulomb repulsion, being referred to as Coulomb exchange. Pauli’s exclusion principle combined with inter-atomic electron hopping additionally leads to kinetic exchange and superexchange. Here we disentangle the different exchange channels in anisotropic Kitaev-Heisenberg context. By quantum chemical computations, we show that anisotropic Coulomb exchange, completely neglected so far in the field, may be as large as (or even larger than) other contributions — kinetic exchange and superexchange. This opens new perspectives onto anisotropic exchange mechanisms and sets the proper conceptual framework for further research on tuning Kitaev-Heisenberg magnetism.

*Introduction.* Magnetism has constantly been a source of new fundamental concepts in solid-state and statistical physics. It is also important to technological applications: many devices around us are (electro)magnetic. Magnetism is typically illustrated through Heisenberg’s textbook model of interacting atomic magnetic moments. Recently, however, it has become clear that for certain magnetic materials Heisenberg’s isotropic interaction picture is not applicable; their behavior can only be described through highly *anisotropic* spin models. The latter may imply completely different interaction strengths for different magnetic-moment projections and, seemingly counterintuitive, directional dependence of the leading anisotropic coupling [1, 2] for symmetry-equivalent pairs of moments. While that opens entire new perspectives in magnetism, provides the grounds for new, exotic states that are now being revealed for the first time, and hints to potential technological applications like quantum computation [1], how such anisotropies arise is not yet fully clarified: we know those may be dominant in particular systems but do not understand in detail the underlying physics and how to tune such interactions in the lab.

Here we shed fresh light on the exchange mechanisms underlying symmetric anisotropic magnetic interactions, both diagonal (i. e., Kitaev [1, 2]) and off-diagonal, by using *ab initio* quantum chemical computational methods. To do so, we exploit the ladder of controlled approximations that quantum chemistry offers: single-configuration schemes, multiconfiguration theory, and multireference configuration-interaction. Honeycomb  $\alpha$ - $\text{RuCl}_3$ , in particular, the relatively high-symmetry crystalline structure recently discovered under a pressure of  $\approx 1.3$  GPa [3], and triangular-lattice  $\text{NaRuO}_2$  [4] were chosen as benchmark Kitaev-Heisenberg material platforms. We establish that a decisive contribution to the Kitaev effective coupling constant  $K$  comes from (anisotropic) Coulomb exchange, a mechanism ignored so far in the literature. In the case of the off-diagonal ( $x$ - $z$ / $y$ - $z$ ) in-

teraction  $\Gamma'$ , which can give rise to spin liquid ground states by itself [5], anisotropic Coulomb exchange is even dominant, as much as  $\sim 90\%$  of the effective coupling parameter computed by multireference configuration-interaction. Our analysis provides unparalleled specifics as concerns  $t_{2g}^5-t_{2g}^5$  Kitaev-Heisenberg magnetic interactions and perspective onto what reliable quantitative predictions would imply: not only controlled *ab initio* approximations to explicitly tackle intersite virtual excitations but also exact Coulomb exchange; the latter is available in self-consistent-field Hartree-Fock theory, the former in post-Hartree-Fock wave-function-based quantum chemical methods.

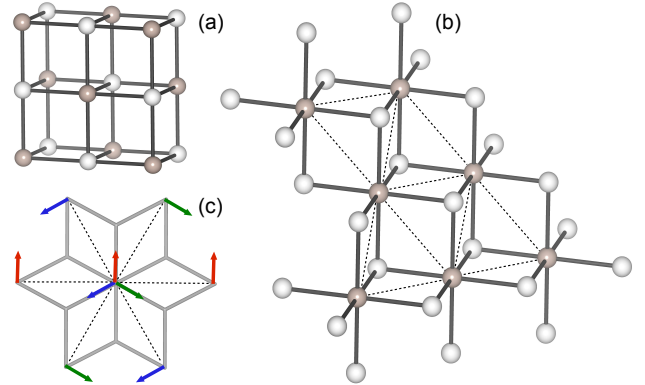


FIG. 1. (a) Rocksalt-type lattice. The M-L bonds are along either  $x$ ,  $y$ , or  $z$ . (b) With two different cation species ( $A$ ,  $B$ ) forming successive layers perpendicular to the  $[111]$  axis, a rhombohedral  $ABL_2$  structure is realized — each layer features a triangular network of edge-sharing octahedra. Honeycomb  $A_2BL_3$  structures are obtained when one of the cation species ( $A$ ) occupies additional sites within the layer of the other ( $B$ ), corresponding to the centers of  $B_6$  hexagonal rings; in  $\alpha$ - $\text{RuCl}_3$ , all  $A$  sites are empty. (c) On each  $B_2L_2$  plaquette (ions not drawn), the Kitaev interaction couples only spin components normal to the respective plaquette. All three spin components are shown only for the central magnetic site.

*Networks of  $M_2L_2$  plaquettes with strong Ising-like anisotropy.* Kitaev magnetism refers to anisotropic magnetic interactions  $K\tilde{S}_i^\gamma\tilde{S}_j^\gamma$  that are ‘bond’ dependent, i.e., for a given pair of adjacent 1/2 pseudospins  $\tilde{\mathbf{S}}_i$  and  $\tilde{\mathbf{S}}_j$ , the easy axis defined through the index  $\gamma$  can be parallel to either  $x$ ,  $y$ , or  $z$  [1]. This can be easily visualized for layered structures of edge-sharing  $ML_6$  octahedra derived from the rocksalt crystalline arrangement (see Fig. 1), either triangular-lattice  $AMO_2$  [6] or honeycomb  $A_2MO_3$  [2] (and  $MCl_3$ ) structures, where M, A, and L are transition-metal, alkaline, and ligand ions, respectively: for each of the magnetic ‘bonds’ emerging out of a given magnetic site M, the easy axis ( $x$ ,  $y$ , or  $z$ ) is normal to the square plaquette defined by two adjacent transition-metal ions and the two bridging ligands. Kitaev’s honeycomb spin model has quickly become a major reference point in quantum magnetism research: it is exactly solvable and yields a quantum spin liquid (QSL) ground state in which the spins fractionalize into emergent Majorana quasiparticles [1]. The latter are neutral self-adjoint fermions that are simultaneously particle and antiparticle. QSL ground states have been experimentally confirmed in the Kitaev-Heisenberg honeycomb systems  $H_3LiIr_2O_6$  [7] and  $\alpha$ - $RuCl_3$  [8, 9] but also in a triangular-lattice magnet with seemingly sizable anisotropic intersite couplings,  $NaRuO_2$  [4].

*Ru–Ru anisotropic exchange.* Having QSL phases materialized on both hexagonal and triangular networks of  $Ru_2L_2$  plaquettes makes Ru quite special. For insights into  $t_{2g}^5-t_{2g}^5$  anisotropic exchange in both  $\alpha$ - $RuCl_3$  and  $NaRuO_2$  crystallographic settings, detailed quantum chemical calculations were carried out for  $Ru_2Cl_{10}$  and  $Ru_2O_{10}$  magnetic units as found in the respective materials. The adjacent in-plane  $RuL_6$  octahedra coordinating those two-octahedra central units were also explicitly included in the quantum chemical computations but using more compact atomic basis sets. Complete-active-space self-consistent-field (CASSCF) optimizations [10, 11] were initially performed with six (Ru  $t_{2g}$ ) valence orbitals and ten electrons as active (abbreviated hereafter as (10e,6o) active space). Subsequently, two other types of wave-functions were generated, using in each case the orbitals obtained from the (10e,6o) CASSCF calculations: (i) single-configuration (SC)  $t_{2g}^5-t_{2g}^5$  (i.e., the  $t_{2g}^4-t_{2g}^6$  and  $t_{2g}^6-t_{2g}^4$  configurations which were accounted for in the initial CASSCF were excluded in this case by imposing appropriate orbital-occupation restrictions) and (ii) multireference configuration-interaction (MRCI) [10, 12] wave-functions having the (10e,6o) CASSCF as kernel and additionally accounting for single and double excitations out of the central-unit Ru  $t_{2g}$  and bridging-ligand valence  $p$  (either O  $2p$  or Cl  $3p$ ) orbitals. By comparing data at these different levels of approximation — SC, CASSCF, and MRCI — it is possible to draw conclusions on the role of various exchange mechanisms. The

TABLE I. Nearest-neighbor magnetic couplings (meV) in high-symmetry  $\alpha$ - $RuCl_3$  [3], results of spin-orbit calculations at various levels of theory. The MRCI is performed having the (10e,6o) CASSCF wave-function as kernel.

	$K$	$J$	$\Gamma_{xy} \equiv \Gamma$	$\Gamma_{yz} = \Gamma_{zx} \equiv \Gamma'$
SC	-1.75	0.35	-0.11	0.42
CASSCF (10e,6o)	-1.73	-1.04	0.89	0.46
MRCI	-3.73	-0.03	1.62	0.45

CASSCF optimization was performed for the lowest nine singlet and lowest nine triplet states associated with the (10e,6o) setting. Those were the states for which spin-orbit couplings (SOCs) were further accounted for [13], at either SC, CASSCF, or MRCI level, which yields in each case a number of 36 spin-orbit states.

A unit of two nearest-neighbor octahedra exhibits  $C_{2h}$  point-group symmetry, in both  $\alpha$ - $RuCl_3$  [3] and  $NaRuO_2$  [4], implying a generalized bilinear effective spin Hamiltonian of the following form for a pair of adjacent 1/2-pseudospins  $\tilde{\mathbf{S}}_i$  and  $\tilde{\mathbf{S}}_j$ :

$$\mathcal{H}_{ij}^{(\gamma)} = J\tilde{\mathbf{S}}_i \cdot \tilde{\mathbf{S}}_j + K\tilde{S}_i^\gamma\tilde{S}_j^\gamma + \sum_{\alpha \neq \beta} \Gamma_{\alpha\beta}(\tilde{S}_i^\alpha\tilde{S}_j^\beta + \tilde{S}_i^\beta\tilde{S}_j^\alpha). \quad (1)$$

The  $\Gamma_{\alpha\beta}$  coefficients denote the off-diagonal components of the  $3 \times 3$  symmetric-anisotropy exchange tensor, with  $\alpha, \beta, \gamma \in \{x, y, z\}$ . The lowest four spin-orbit eigenstates from the *ab initio* quantum chemical output (eigenvalues lower by  $\sim 0.2$  eV with respect to the eigenvalues of higher-lying excited states) are mapped for each different set of calculations onto the eigenvectors of the effective spin Hamiltonian (1), following the procedure described in refs. [14, 15]: those four expectation values and the matrix elements of the Zeeman Hamiltonian in the basis of the four lowest-energy spin-orbit eigenvectors are put in direct correspondence with the respective eigenvalues and matrix elements of (1).

Nearest-neighbor effective magnetic couplings as obtained at three different levels of theory (SOC included) for  $\alpha$ - $RuCl_3$  are listed in Table I. A very interesting finding is the vanishingly small  $J$  value in the spin-orbit MRCI computations, which yields a fully anisotropic  $K$ - $\Gamma$ - $\Gamma'$  effective magnetic model for the nearest-neighbor magnetic interactions and in principle increases the chances of realizing a QSL ground state. This particular aspect will be discussed elsewhere.

Even more remarkable are the large anisotropic Coulomb exchange contributions obtained by SC calculations with SOC. The diagonal Kitaev coupling  $K$ , for example, is basically the same at the lowest two levels of approximation (first column in Table I), SC (only the  $t_{2g}^5-t_{2g}^5$  electron configuration considered) and CASSCF (10e,6o) ( $t_{2g}^5-t_{2g}^5$ ,  $t_{2g}^4-t_{2g}^6$ , and  $t_{2g}^6-t_{2g}^4$  configurations treated on the same footing, where the latter type of states bring kinetic  $Ru(t_{2g})$ - $Ru(t_{2g})$  exchange). This

indicates that intersite  $\text{Ru } t_{2g} \rightarrow \text{Ru } t_{2g}$  excitations (i.e., kinetic exchange) do not really affect  $K$ . What matters as concerns the size of the Kitaev coupling are (i) Coulomb exchange, with a contribution of  $-1.75$  meV, and (ii) excitations to higher-lying states and so called dynamical correlation effects [10] accounted for in MRCI, with a contribution of  $-2$  meV. Part of (ii) corresponds to Ru-Cl-Ru superexchange [16, 17], involving also the Ru  $4d e_g$  levels [2, 18, 19]. Especially striking is the diagnosis carried out for the off-diagonal  $\Gamma'$  effective interaction parameter: out of a spin-orbit MRCI value of  $0.45$  meV,  $0.42$  corresponds to anisotropic Coulomb exchange. A pictorial representation of the various contributions to  $K$ ,  $J$ ,  $\Gamma$ , and  $\Gamma'$  in high-symmetry  $\alpha\text{-RuCl}_3$  [3] is provided in Fig. 2.

MRCI+SOC computations for adjacent edge-sharing  $\text{RuO}_6$  octahedra in triangular-lattice  $\text{NaRuO}_2$  indicate that the largest nearest-neighbor coupling parameter is the isotropic Heisenberg  $J$ ,  $-5.2$  meV; the other effective interactions,  $K$ ,  $\Gamma$ , and  $\Gamma'$ , amount to  $2$ ,  $3.6$ , and  $1.1$  meV, respectively, by spin-orbit MRCI. For better visualization, since the most important anisotropic Coulomb exchange contributions arise also in this system for  $K$  and  $\Gamma'$ , we depict in Fig. 3 only the structure of these two magnetic couplings and omit the  $J$  and  $\Gamma$  effective interactions, which have significantly larger absolute values. Plots for the latter are provided in Supplemental Material (SM). It is seen that anisotropic Coulomb exchange represents the second largest contribution to the Kitaev  $K$  and the leading underlying mechanism in the case of  $\Gamma'$ .

Anisotropic Coulomb exchange as found in the SC calculation (also referred to as direct exchange [16]) repre-

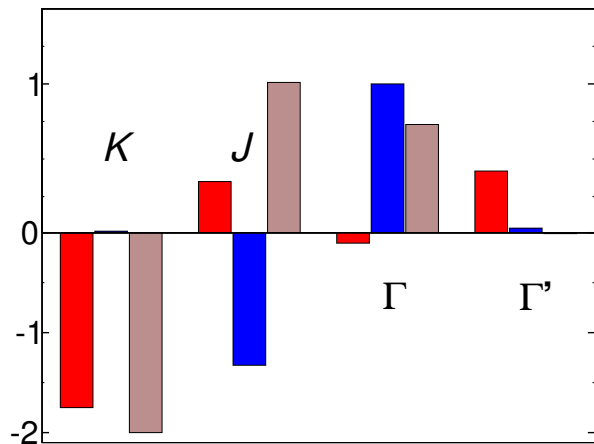


FIG. 2. Exchange contributions to the intersite effective magnetic couplings in high-symmetry  $\alpha\text{-RuCl}_3$  [3]: Coulomb exchange (SC results, in red),  $\text{Ru}(t_{2g})\text{-Ru}(t_{2g})$  kinetic exchange (as the difference between CASSCF and SC data, in blue), plus contributions related to Ru-Cl-Ru superexchange [16–19] and so called dynamical correlation effects [10] (as the difference between MRCI and CASSCF, in brown).

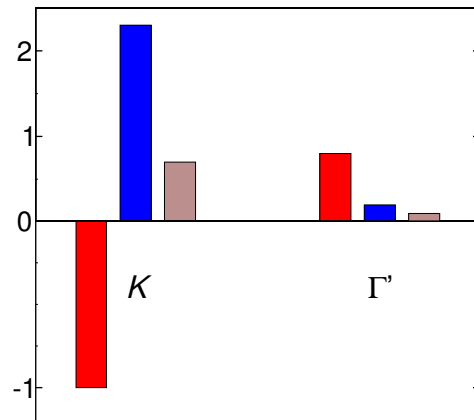


FIG. 3. Exchange contributions to  $K$  and  $\Gamma'$  in  $\text{NaRuO}_2$  [4]: Coulomb exchange (SC results, in red),  $\text{Ru}(t_{2g})\text{-Ru}(t_{2g})$  kinetic exchange (as the difference between CASSCF and SC data, in blue), plus contributions related to Ru-O-Ru superexchange and dynamical correlations (as the difference between MRCI and CASSCF, in brown).

sents genuine new physics, not addressed so far in the literature. Finding that up to  $\sim 45\%$  of the Kitaev effective coupling constant  $K$  has to do with Coulomb exchange and that the off-diagonal anisotropic coupling  $\Gamma'$ , which may give rise to spin-liquid ground states by itself [5], comes more than  $90\%$  from Coulomb exchange (last column in Table I) obviously challenges present views and notions in Kitaev-Heisenberg quantum magnetism research. This is just another example illustrating the need for *ab initio* quantum chemical methods in order to achieve even a qualitatively correct picture of the essential underlying physics. Recent quantum chemical results that lead to the same conclusion refer to the role of fluctuations involving the third and fourth electronic shells in renormalizing antiferromagnetic interactions in copper oxide compounds [20].

To provide additional reference points, we computed the isotropic Coulomb exchange integrals (i.e., without accounting for SOC) for different distributions of the Ru  $t_{2g}$  holes in the  $t_{2g}^5\text{-}t_{2g}^5$  arrangement. For holes in plaquette-plane  $4d$  orbitals having overlapping lobes along the Ru-Ru axis (i.e., for  $xy$ -like  $t_{2g}$  functions), for example, the Coulomb exchange integral amounts to  $-25.4$  meV. For comparison, in  $3d^9$  copper oxide compounds with corner-sharing ligand octahedra, the Coulomb exchange matrix element is in the region of  $-10$  meV (from SC  $d_{x^2-y^2}^1\text{-}d_{x^2-y^2}^1$  calculations) [21, 22]. Being aware of experimental estimates of  $100\text{--}150$  meV for the Heisenberg  $J$ , an isotropic Coulomb exchange contribution of  $-10$  meV can be neglected in layered cuprates. Yet, this does not seem to be the case for  $t_{2g}^5$  edge-sharing octahedra.

The full  $3\times 3$  matrix for adjacent Ru  $t_{2g}^5$  sites ( $i, j$ ) in high-symmetry  $\text{RuCl}_3$  is provided in Table II. How exactly SOC and Coulomb interactions commix to yield

TABLE II. Coulomb exchange (in meV) for Ru  $t_{2g}$  holes in RuCl<sub>3</sub>  $t_{2g}^5-t_{2g}^5$  arrangement, obtained in each case as the difference between triplet ( $d_{i,\alpha}^\uparrow d_{j,\beta}^\uparrow$ ,  $\alpha, \beta \in \{xy, yz, zx\}$ ) and singlet ( $d_{i,\alpha}^\uparrow d_{j,\beta}^\downarrow$ ) energies.

	$d_{xy}$	$d_{yz}$	$d_{zx}$
$d_{xy}$	-25.4	-4.7	-4.7
$d_{yz}$	-4.7	-0.6	-7.0
$d_{zx}$	-4.7	-7.0	-0.6

large *anisotropic* Coulomb exchange integrals remains to be analyzed in detail in future work. The important point however is that, at the  $t_{2g}^5-t_{2g}^5$  SC level, there is a Coulomb exchange matrix element for each possible pair of holes —  $d_{xy}-d_{xy}$ ,  $d_{xy}-d_{yz}$  etc. SOC mixes up those different Slater determinants, and the resulting spin-orbit wave-functions are not spin eigenstates. The spin-orbit level structure in the two-octahedra problem can be reduced to an effective pseudospin model only by introducing anisotropic Coulomb exchange matrix elements (i. e., the SC values provided in Table I).

*Conclusions.* To summarize, we resolve the exchange mechanisms giving rise to anisotropic magnetic interactions in hexagonal and triangular networks of edge-sharing RuL<sub>6</sub>  $t_{2g}^5$  octahedra. Different from present assumptions and exchange models relying exclusively on inter-atomic hopping processes, the quantum chemical analysis indicates major Coulomb-exchange contributions, to both  $K$  and  $\Gamma'$ . These findings redefine the conceptual frame within which Kitaev magnetism should be addressed. Also, in light of the *ab initio* quantum chemical data, various estimates, interpretations, and predictions based only on kinetic-exchange and superexchange models might require reevaluation — what is represented in red color in Figs. 2 and 3 is simply ignored in existing effective-model theories and studies.

*Acknowledgments.* P. B., T. P., and L. H. acknowledge financial support from the German Research Foundation (Deutsche Forschungsgemeinschaft, DFG), projects 441216021 and 468093414, and technical assistance from U. Nitzsche. We thank J. Geck, G. Khaliullin, S. Winter, O. Janson, S. D. Wilson, and U. K. Rößler for discussions.

- [2] G. Jackeli and G. Khaliullin, *Phys. Rev. Lett.* **102**, 017205 (2009).
- [3] Q. Stahl, T. Ritschel, G. Garbarino, F. Cova, A. Isaeva, T. Doert, and J. Geck, arXiv:2209.08367 (2022).
- [4] B. R. Ortiz, P. M. Sarte, A. H. Avidor, A. Hay, E. Kenney, A. I. Kolesnikov, D. M. Pajerowski, A. A. Aczel, K. M. Taddei, C. M. Brown, C. Wang, M. J. Graf, R. Seshadri, L. Balents, and S. D. Wilson, *Nat. Phys.* (2023), 10.1038/s41567-023-02039-x.
- [5] I. Rousochatzakis and N. B. Perkins, *Phys. Rev. Lett.* **118**, 147204 (2017).
- [6] A. J. W. Reitsma, L. F. Feiner, and A. M. Oleś, *New J. Phys.* **7**, 121 (2005).
- [7] K. Kitagawa, T. Takayama, Y. Matsumoto, A. Kato, R. Takano, Y. Kishimoto, S. Bette, R. Dinnebier, G. Jackeli, and H. Takagi, *Nature* **554**, 341 (2018).
- [8] A. Banerjee, J. Yan, J. Knolle, C. A. Bridges, M. B. Stone, M. D. Lumsden, D. G. Mandrus, D. A. Tennant, R. Moessner, and S. E. Nagler, *Science* **356**, 1055 (2017).
- [9] S.-H. Baek, S.-H. Do, K.-Y. Choi, Y. S. Kwon, A. U. B. Wolter, S. Nishimoto, J. van den Brink, and B. Büchner, *Phys. Rev. Lett.* **119**, 037201 (2017).
- [10] T. Helgaker, P. Jørgensen, and J. Olsen, *Molecular Electronic Structure Theory* (John Wiley & Sons, Chichester, 2000).
- [11] D. A. Kreplin, P. J. Knowles, and H.-J. Werner, *J. Chem. Phys.* **152**, 074102 (2020).
- [12] P. J. Knowles and H.-J. Werner, *Theor. Chim. Acta* **84**, 95 (1992).
- [13] A. Berning, M. Schweizer, H.-J. Werner, P. J. Knowles, and P. Palmieri, *Mol. Phys.* **98**, 1823 (2000).
- [14] N. A. Bogdanov, V. M. Katukuri, J. Romhányi, V. Yushankhai, V. Kataev, B. Büchner, J. van den Brink, and L. Hozoi, *Nat. Commun.* **6**, 7306 (2015).
- [15] R. Yadav, N. A. Bogdanov, V. M. Katukuri, S. Nishimoto, J. van den Brink, and L. Hozoi, *Sci. Rep.* **6**, 37925 (2016).
- [16] P. W. Anderson, *Phys. Rev.* **115**, 2 (1959).
- [17] J. Kanamori, *J. Phys. Chem. Solids* **10**, 87 (1959).
- [18] J. Chaloupka, G. Jackeli, and G. Khaliullin, *Phys. Rev. Lett.* **105**, 027204 (2010).
- [19] S. M. Winter, Y. Li, H. O. Jeschke, and R. Valentí, *Phys. Rev. B* **93**, 214431 (2016).
- [20] N. A. Bogdanov, G. L. Manni, S. Sharma, O. Gunnarsson, and A. Alavi, *Nat. Phys.* **18**, 190 (2022).
- [21] R. L. Martin, *J. Chem. Phys.* **98**, 8691 (1993).
- [22] A. van Oosten, R. Broer, and W. Nieuwpoort, *Chem. Phys. Lett.* **257**, 207 (1996).

[1] A. Kitaev, *Ann. Phys.* **321**, 2 (2006).

# Supplemental Material — Anisotropic Coulomb exchange as source of Kitaev and off-diagonal symmetric anisotropic couplings

Pritam Bhattacharyya,<sup>1</sup> Thorben Petersen,<sup>1</sup> Nikolay A. Bogdanov,<sup>2</sup> and Liviu Hozoi<sup>1</sup>

<sup>1</sup>*Institute for Theoretical Solid State Physics, Leibniz IFW Dresden, Helmholtzstraße 20, 01069 Dresden, Germany*

<sup>2</sup>*Max Planck Institute for Solid State Research, Heisenbergstraße 1, 70569 Stuttgart, Germany*

(Dated: July 3, 2023)

Different from the vast majority of Kitaev-Heisenberg honeycomb systems, only one type of Ru-Ru link is present in both  $\alpha$ -RuCl<sub>3</sub> at  $p=1.26$  GPa [1] and NaRuO<sub>2</sub> [2]. Since a unit of two nearest-neighbor octahedra exhibits  $C_{2h}$  point-group symmetry, the relevant bilinear effective spin Hamiltonian for a pair of adjacent 1/2-pseudospins  $\tilde{\mathbf{S}}_i$  and  $\tilde{\mathbf{S}}_j$  reads

$$\mathcal{H}_{ij}^{(\gamma)} = J\tilde{\mathbf{S}}_i \cdot \tilde{\mathbf{S}}_j + K\tilde{S}_i^\gamma \tilde{S}_j^\gamma + \sum_{\alpha \neq \beta} \Gamma_{\alpha\beta} (\tilde{S}_i^\alpha \tilde{S}_j^\beta + \tilde{S}_i^\beta \tilde{S}_j^\alpha). \quad (\text{S1})$$

The  $\Gamma_{\alpha\beta}$  coefficients denote the off-diagonal components of the  $3 \times 3$  symmetric-anisotropy exchange tensor, with  $\alpha, \beta, \gamma \in \{x, y, z\}$ . An antisymmetric Dzyaloshinskii-Moriya coupling is not allowed, given the inversion center.

The lowest four expectation values obtained from the quantum chemical calculations (either SC, CASSCF, or MRCI level) for both compounds (NaRuO<sub>2</sub> and high-symmetry  $\alpha$ -RuCl<sub>3</sub>) and the matrix elements of the Zeeman Hamiltonian in the basis of the four lowest-energy spin-orbit eigenvectors are put in direct correspondence with the respective eigenvalues and matrix elements of (S1). Having two of the states in the same irreducible representation of the  $C_{2h}$  point group, such one-to-one mapping translates into two possible sets of effective magnetic couplings. The relevant array is chosen as the one whose  $g$  factors fit the  $g$  factors corresponding to a single RuCl<sub>6</sub> (RuO<sub>6</sub>)  $t_{2g}^5$  octahedron.

We used the standard coordinate frame usually employed in the literature, different from the rotated frame employed in earlier quantum chemical studies [3–5] that affects the sign of  $\Gamma$  (see also footnote [48] in Ref. [6]). The SC label in Table I in the main text indicates a CASCI in which intersite excitations are not considered. This is also referred to as occupation-restricted multiple active space (ORMAS) scheme [7].

We employed relativistic pseudopotentials (ECP28MDF) and BSs (ECP28MDF-VTZ) [8] for the central Ru species. All-electron BSs of quintuple- $\zeta$  quality were utilized for the two bridging ligands [9] and of triple- $\zeta$  quality for the remaining eight Cl anions [9] linked to the two octahedra of the reference unit. The four adjacent cations were represented as closed-shell Rh<sup>3+</sup>  $t_{2g}^6$  species, using the same pseudopotentials (Ru ECP28MDF) and BSs (Ru ECP28MDF-VDZ [3s3p3d]) [8] considered for the single-octahedron computations;

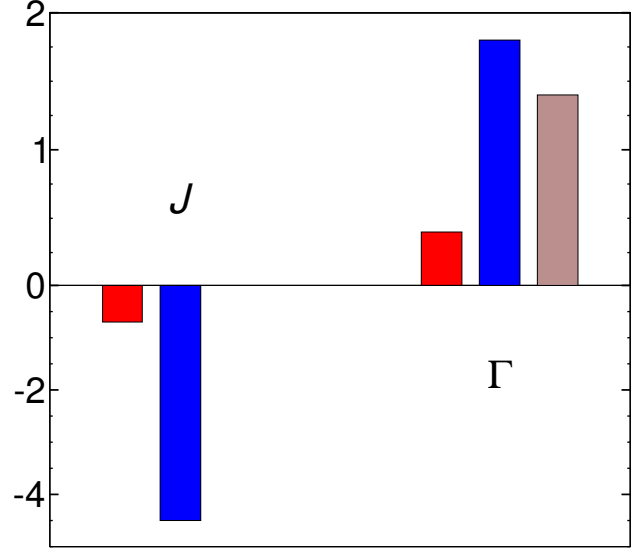


FIG. S1. Exchange contributions to  $J$  and  $\Gamma$  in NaRuO<sub>2</sub> [2]: Coulomb exchange (SC results, in red), Ru( $t_{2g}$ )-Ru( $t_{2g}$ ) kinetic exchange (as the difference between CASSCF and SC data, in blue), plus contributions related to Ru-O-Ru superexchange and dynamical correlations (as the difference between MRCI and CASSCF, in brown); the brown contribution of  $J$  is zero.

the outer 16 Cl ligands associated with the four adjacent octahedra were described through minimal ANO BSs [10].

To derive the inter-site effective magnetic couplings of NaRuO<sub>2</sub>, clusters with two edge-sharing RuO<sub>6</sub> octahedra in the central region were considered. The eight in-plane octahedra directly linked to the two octahedra central unit and 22 nearby Na ions were also explicitly included in the quantum chemical computations but using much more compact basis sets. We utilized energy-consistent relativistic pseudopotentials (ECP28MDF) and Gaussian-type valence basis sets of effective quadruple- $\zeta$  quality (ECP28MDF-VTZ) for the central Ru species [8]. All-electron basis sets of quintuple- $\zeta$  quality were employed for the two bridging ligands [11] while all-electron basis sets of triple- $\zeta$  quality were applied for the remaining eight O anions [11] associated with the two octahedra of the reference unit. The eight adjacent transition-metal (TM) cations were represented as closed-shell Rh<sup>3+</sup>  $t_{2g}^6$  species, using non-

relativistic pseudopotentials (Ru ECP29MHF) and (Ru ECP28MHF) (8s7p6d)/[4s3p2d] basis sets [12, 13]; the outer 22 O ligands associated with the eight adjacent octahedra were described through minimal all-electron atomic-natural-orbital (ANO) basis sets [10]. Large-core pseudopotentials were considered for the 22 Na nearby cations [14].

- 
- [1] Q. Stahl, T. Ritschel, G. Garbarino, F. Cova, A. Isaeva, T. Doert, and J. Geck, arXiv:2209.08367 (2022).
- [2] B. R. Ortiz, P. M. Sarte, A. H. Avidor, A. Hay, E. Kenney, A. I. Kolesnikov, D. M. Pajeroski, A. A. Aczel, K. M. Taddei, C. M. Brown, C. Wang, M. J. Graf, R. Seshadri, L. Balents, and S. D. Wilson, *Nat. Phys.* (2023), [10.1038/s41567-023-02039-x](https://doi.org/10.1038/s41567-023-02039-x).
- [3] R. Yadav, N. A. Bogdanov, V. M. Katukuri, S. Nishimoto, J. van den Brink, and L. Hozoi, *Sci. Rep.* **6**, 37925 (2016).
- [4] S. Nishimoto, V. M. Katukuri, V. Yushankhai, H. Stoll, U. K. Röbler, L. Hozoi, I. Rousochatzakis, and J. van den Brink, *Nat. Commun.* **7**, 10273 (2016).
- [5] R. Yadav, M. S. Eldeeb, R. Ray, S. Aswartham, M. I. Sturza, S. Nishimoto, J. van den Brink, and L. Hozoi, *Chem. Sci.* **10**, 1866 (2019).
- [6] L. Janssen, E. C. Andrade, and M. Vojta, *Phys. Rev. B* **96**, 064430 (2017).
- [7] J. Ivanic, *J. Chem. Phys.* **119**, 9364 (2003).
- [8] K. A. Peterson, D. Figgen, M. Dolg, and H. Stoll, *J. Chem. Phys.* **126**, 124101 (2007).
- [9] D. E. Woon and T. H. Dunning Jr., *J. Chem. Phys.* **98**, 1358 (1993).
- [10] K. Pierloot, B. Dumez, P.-O. Widmark, and B. O. Roos, *Theor. Chim. Acta* **90**, 87 (1995).
- [11] T. H. Dunning, *J. Chem. Phys.* **90**, 1007 (1989).
- [12] D. Andrae, U. Haeussermann, M. Dolg, H. Stoll, and H. Preuss, *Theor. Chim. Acta* **77**, 123 (1990).
- [13] J. M. L. Martin and A. Sundermann, *J. Chem. Phys.* **114**, 3408 (2001).
- [14] P. Fuentealba, H. Preuss, H. Stoll, and L. Von Szentpály, *Chem. Phys. Lett.* **89**, 418 (1982).